INFLUENCE OF NANOPARTICLES ADDITIVIES ON MECHANICAL PROPERTIES OF FABRIC REINFORCED COMPOSITES

T. Suchý[1], K. Balík[2], Z. Sucharda[2], M. Černy[2], M. Sochor[1]

[1] Czech Technical University in Prague,
Faculty of Mechanical Engineering,
Laboratory of Biomechanics, Prague, Czech Republic
[2] Institute of Rock Structure and Mechanics,
Czech Academy of Sciences, Department of Composites and Carbon Materials, Prague, Czech Republic
*E-mail:suchyt@biomed.fsid.cvut.cz

[Engineering of Biomaterials, 69-72, (2007), 1-2]

Introduction

For construction of artificial bone substitutes, several materials have been used. Each of these material types has its specific advantages and limitations. It is important to match their mechanical and other chemical and physical properties. From a wide range of studies performed on various materials it follows that the bone tissue formation is influenced by several factors; porosity, wettability, chemical composition, rigidity etc. [1,2]. This study objection is to present the influence of hydroxyapatite nanoparticles additives, commonly used to improve the bioactivity of implants, on mechanical properties (namely flexural strength and flexural modulus) of composite material potentially applicable in bone surgery [3,4].

Materials and methods

A composite material based on fabric reinforcement (Aramid balanced fabric, based on aromatic polyamide fibers HM 215, Hexcel, France) and polysiloxane matrix M130 (Lucebni zavody Kolin, Czech Republic) was prepared; see TABLE 1 and FIGURE 1.

	Aramid
Monofile diameter [μm]	12
density [g/cm^3]	1.44
Tensile strength [MPa]	3150
Young modulus [GPa]	110

TABLE 1. Monofile properties of fabric used.

Hydroxyapatite (HAp) powder, particle size avg. 20-70 nm, was added into the matrix before impregnation in the amount of 0, 2, 5, 10, 15, 20 and 25wgt% (HAp/matrix) (BABI-HAP-N20 AH, grains in ammonium hydroxyde suspension Berkeley Advanced Biomaterials Inc., San Leandro, CA, USA), see FIG.2.

For this purpose, the homogenizer DI 18 Basic (IKA Werke GMbH) was used. A weighted amount of HAp was gradually inserted into a weighted amount of polysiloxane matrix M130, so that uniform dispersion of the HAp filler in the matrix (running speed of the homogenizer 17 500 1/min, dispersion time 6 hours) was achieved.

After this procedure, the fabric was impregnated by the matrix/Hap blend and then, after 24 hours, cut into squared pieces with dimensions 118x118mm. 11 impregnated layers

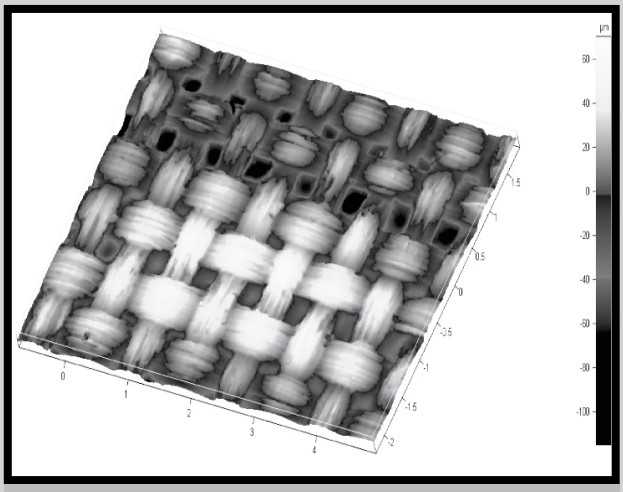

FIG.1. 3D picture of aramid fabric 20796 (measured by MarSurf TS 50/4 optical equipment, Mahr, Germany).

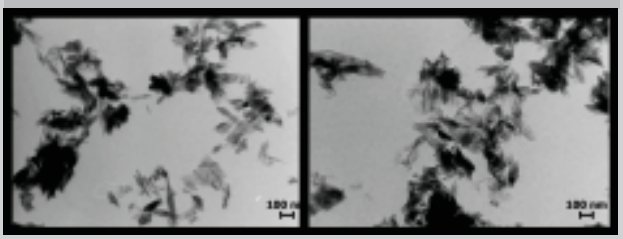

FIG.2. TEM pictures of agglomerated needle-shaped nano HAp.

were placed into the curing form with respect to the axis of fibers (each layer has a same orientation of the warp, with ply direction (0°) and the fill, with ply direction (90°)). The green composite was heated in the form at the temperature 135°C for two hours and then cured under pressure 1.1MPa at the temperature 225°C in air atmosphere for 4.5 hours and finally hardened without applying the pressure at the temperature 250°C for 4 hours. This pressing cycle corresponds to an observed temperature viscosity rise of the matrix used. After curing, cured plates were cut with diamond saw to appropriate size according to further 4-point bending mechanical tests (see below).

Flexural strength (R_{fM}) and flexural modulus (E_f) in the direction of the fiber axis were determined by a four-point bending setup in an Inspekt 100HT material tester (Hagewald & Peschke, Germany) with respect to ISO 14125, 10 samples from each group were measured with dimensions 60x2.5x15mm (length x thickness x width), crosshead speed 0.5mm/min, load cell HT Beige 2kN, Maytec Germany.

Results

Seven kinds of composite samples differing by HAp volume were examined. The open porosity and apparent density of all composite samles were measured according to ASTM C-373 (TABLE 2).

The flexure strength (flexure modulus)/HAp volume faction relationship were determined - FIG.3). The presence of HAp in composite matrix has, in general, a negative influence on mechanical properties (possibly due to a lower cohesion between layers). This fact can be favourable when looking for a sufficient compromise between mechanical properties comparable with those of human cortical bone and sufficient osseoconductivity. Higher volumes of HAp matrix additives (20, 25%) possibly influence the structure

wgt% (HAp/matrix)	porosity [%]	bulk density [g/cm^3]
0	14.54	1.18
2	18.03	1.12
5	17.84	1.14
10	15.36	1.19
15	14.30	1.28
20	12.09	1.36
25	14.32	1.32

TABLE 2. The open porosity and apparent density of composite samples.

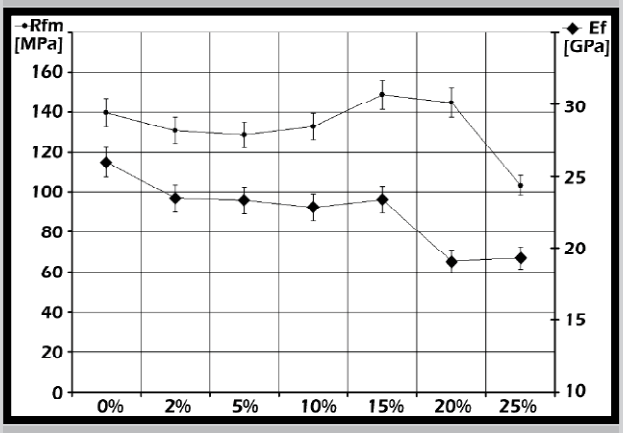

FIG.3. Flexure strength R_{fm} and flexure modulus E_f of composites with HAp nanopartricles.

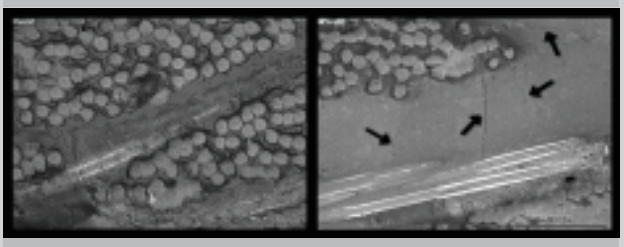

FIG.4. Pictures of polished cross-section of composite with 5% HAp (left) and 20% HAp (right) illustrate multiple cracking in cured matrix with higher amount of HAp.

of cured matrix (FIG.4). In this case, the matrix seems to be prone to a brittle failure (becoming more ceramic), which could lead to a lower resistance to fatigue failure, which is one of limiting factors for applicability of implant materials.

Conclusions

We obtained flexure strength and flexure modulus of composites based on aramid fabric and polysiloxane resin with various amount of HAp nanoparticles additives. It is important to match the compromise between sufficient mechanical properties and amount of bioactive additives. It seems that higher amount of additives should have a negative influence on mechanical properties. As a further step it will be necessary to define an amount of additives more precisely (step 1-2%) and also to compare different size of particles (nano vs. micro).

Acknowledgements

This study was supported by the Czech Science Foundation under the project No. 106/06/1576 and by the Ministry of Education of Czech Republic project No. MSM 6840770012.

References

[1] Ramakrishna, S., Mayer, J., Wintermantel, E. Composite Science and Technology, 61, 2001. pp. 1189-1224.
[2] Nakamura et al. Journal of Biomedical Materials Research, 19, 1985, pp. 685-698.
[3] Suchy, T., Balík, K., Sochor, M., Černý, M., Hulejová, H. et al. In: Human Biomechanics 2006 [CD-ROM]. University of Technology, Brno, 2006, pp. 1-5.
[4] Balik, K., Sochor, M., Suchy, T.Cerny, M., Hulejova, H. In: Journal of Biomechanics, Abstracts of the 5th World Congress of Biomechanics, Munich, Germany, Berlin: Elsevier, 2006, p. S264.

ANALYSIS OF A CONTACT STRESS DISTRIBUTION IN NEW SHAPE OF A HIP CUP

Jan Sykora*, Svatava Konvickova, Matej Daniel

Laboratory of Human Biomechanics, Department of Mechanics, CTU in Prague, Czech Republic
Laboratory of Human Biomechanics, CTU in Prague, Faculty of Mechanical Engineering, Department of Mechanics, Technicka 4, 166 07, Prague 6, Czech Republic
*E-mail: J.Sykora@sh.cvut.cz

[Engineering of Biomaterials, 69-72, (2007), 2-3]

Introduction

We develop a new design of an acetabular component for a total replacement of a hip joint. We indicate on the basis of the comparison our results of mathematical and finite element models of a contact stress distribution, that it is possible to use the finite element method for the modeling of the non-weigh bearing part of the total replacement of the hip joint. The point of this technical solution of the new hip cup is to design such a shape of the joint surface that will be symmetrical towards the hip joint stress. The shape is designed as the basic mathematical models of the distribution of the contact stress [1]. Three basic forms of this shape were designed. The cup with the hole was chose as the most suitable [2].

Materials and methods

We compared two various finite element models of the hip cup, cup with hole (A) and cup with hole and fillet edges (B). The models were loaded by five forces. We got contact stress distribution between the head and the modified hip cup. The each of those forces had different value and different direction of a loading. The forces matched values of a resultant hip joint force in hip joint in the course of different movement of a human body.

Results

The resultant contact stress distributions are on the FIGURES 1-5. The resultant contact stress distributions for each model at loading of a first force are in FIGURE 1, for second force in FIGURE 2, for third force in FIGURE 3, for fourth force in FIGURE 4 and in FIGURE 5 for last force.